Catalysis Letters 69 (2000) 11–16

Oxidation state of bimetallic PdCu catalysts during liquid phase nitrate reduction

Andrea Edelmann [a], Walter Schießer [a], Hannelore Vinek [a] and Andreas Jentys [b,*]

[a] *Institut für Physikalische und Theoretische Chemie, Technische Universität Wien, Getreidemarkt 9/156, A-1060 Wien, Austria*
E-mail: andreas.jentys@ch.tum.de
[b] *Lehrstuhl für Technische Chemie II, Technische Universität München, Lichtenbergstrasse 4, D-85747 Garching, Germany*

Received 26 June 2000; accepted 30 June 2000

The oxidation state and the structural properties of Al_2O_3-supported bimetallic PdCu catalysts during the catalytic reduction of KNO_3 carried out in the aqueous phase were investigated by X-ray absorption spectroscopy. Under reaction conditions the noble metal component (Pd) was in a reduced state, while the less noble metal (Cu) was found to be partially oxidized. A PdCu phase was formed in the bimetallic catalysts, which appears to be located in small domains on the surface of Pd rich particles.

Keywords: PdCu/Al_2O_3, *in situ* XANES, EXAFS, nitrate reduction, aqueous phase

1. Introduction

Physico-chemical methods for the removal of nitrates from aqueous solutions, especially at concentration levels that cannot be treated with biological denitrification methods, are receiving widespread attention today [1,2]. One of the most attractive processes is the catalytic liquid phase hydrogenation over metal-oxide-supported bimetallic catalysts, which typically consist of a combination between a noble and a non-noble metal. In these catalysts Pd is used for the reduction of nitrite to nitrogen, while bimetallic combinations such as PdCu, PdSn and PdIn are required for the nitrate reduction [3–7]. The catalytic properties of the materials and the reaction conditions were extensively studied, however, information on the structural and chemical properties of the metal components in the working catalysts is limited [8,9] and, in particular, the characterization of the catalyst in the aqueous phase under reaction conditions was not reported so far. The structural and chemical properties of (metal) catalysts are typically affected by the presence of reactant molecules and the surrounding reaction media and, therefore, the characterization of the catalysts in the aqueous phase under reaction conditions is indispensable to improve the understanding of the catalytic reaction.

X-ray absorption spectroscopy (XAS) is among the methods most frequently used to analyze structural and chemical properties of metal components in bimetallic catalysts [10–12]. Although the experiments can be carried out for samples in the liquid phase [13–15], the structural properties of PdCu catalysts were investigated so far only after reduction in the gas phase [9,16–18].

In this study we report the characterization of the chemical and structural properties of bimetallic PdCu/Al_2O_3 catalysts by *in situ* X-ray absorption spectroscopy. The main focus of the experiments was to closely reflect the typical catalyst preparation and reaction conditions during the XAS experiments and to study the catalyst directly in the aqueous phase.

2. Experimental

2.1. Sample preparation

γ-Al_2O_3 (Sigma Aldrich ALOX560C, specific surface area 155 $m^2\,g^{-1}$) was used as support for mono- and bimetallic Cu/Al_2O_3, Pd/Al_2O_3 and PdCu/Al_2O_3 catalysts. Aqueous solutions of $Cu(NO_3)_2$ and $PdNO_3$ were used for the (co-)impregnation. The metal loading of the catalysts was 5 wt% Pd and/or 1.25 wt% Cu. After preparation the catalysts were dried at 323 K for 12 h and calcined in dry air at 773 K for 3 h.

2.2. X-ray absorption spectroscopy

X-ray absorption spectra were measured in Hasylab at DESY (Hamburg, Germany) at beamline X1 (RÖMO II) using Si(311) crystals in the monochromator. The energy resolution was approximately 1 eV at the Cu K edge (8.979 keV) and 3 eV at the Pd K edge (24.35 keV). To calibrate the energy of the monochromator a foil of the corresponding metal was inserted between the second and a third ionization chamber.

In the first series of experiments the samples were prepared as self-supporting wafers and investigated before and after reduction with H_2 in the gas phase using a stainless-steel cell equipped with capton windows [19]. The weight of the samples was chosen to result in a total absorption

---

[*] To whom correspondence should be addressed.

of $\mu x = 2.5$ for the reduced catalysts in order to optimize the signal to noise ratio [20]. The catalysts were reduced in H_2 at 773 K for 30 min (heating rate from room temperature 20 $\mathrm{K\,min^{-1}}$) and after cooling the samples to liquid nitrogen temperature the X-ray absorption spectra were recorded.

In the second series of experiments the catalysts were directly investigated in the aqueous solution. The nitrate reduction reaction was carried out at 298 K in a stirred batch reactor (750 ml volume, operated as a CSTR) containing 75 mg KNO_3 and 0.75 g of the catalyst. H_2 and CO_2 (to compensate the increase in the pH value during the reaction) with flow rates of 200 $\mathrm{ml\,min^{-1}}$ were passed through the reactor. X-ray absorption spectra were measured from the pre-reduced catalysts suspended in H_2O, after introducing the H_2 flow for 60 min at 298 K and after 60 min of reaction in the presence of KNO_3 and CO_2. During all procedures the catalyst remained inside the aqueous reaction media and a contact to the atmosphere was prevented using polyethylene windows to seal the cell against the environment. The cell used for the transmission experiments in the aqueous phase was built from polyamide and consisted of three parts. The two inner parts were formed like a piston and allowed selection of the thickness of the aqueous layer exposed to the X-ray beam in order to adjust the absorption according to the composition of the sample and the energy of the absorption edge being studied. The third part was used to seal the cell against the atmosphere and contained the inlet and outlet for the reactant solution. A peristaltic pump was used to transfer the aqueous solution into the cell, which contained a porous filter to retard the catalyst particles until the desired amount of material was collected. Subsequently, the cell was detached from the reaction setup and inserted into a liquid nitrogen cooled block where the spectra were measured at low temperature. The catalyst mass and the thickness of the aqueous layer were chosen to obtain a total absorption of $\mu x = 2.5$.

In contrast to the other liquid phase cells described in the literature [13–15], our cell design allows an easy adjustment of the thickness of the liquid layer exposed to the X-ray beam. At the energy of the Pd K edge (24.35 keV) the absorption cross section of water is relatively low and, therefore, an aqueous layer of 10 mm thickness resulted in a contribution of ~20% to the total absorption. In contrast, at the energy of the Cu K edge (8.979 keV) an aqueous layer of only 2 mm thickness caused already a contribution of more than 50% to the total absorption coefficient. Therefore, only a tenth of the amount of solid sample could be used for the experiments on the Cu K edge compared to the Pd K edge, which is reflected in the significantly lower signal–noise ratio for the spectra measured at the Cu K edge.

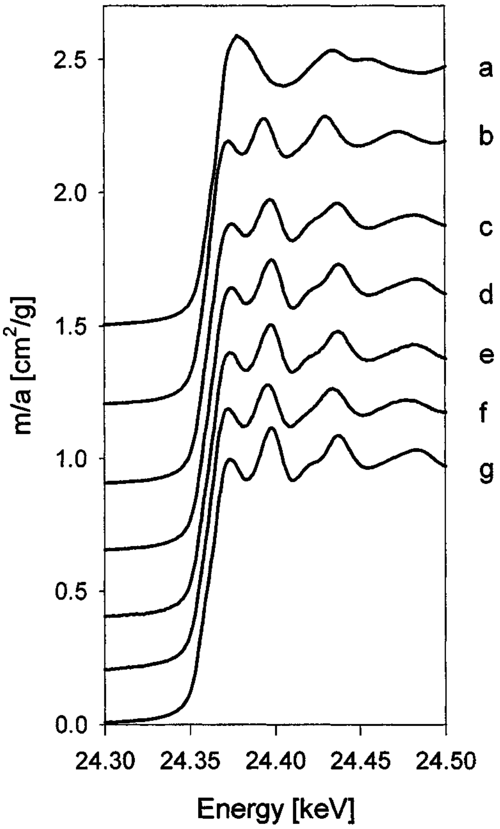

Figure 1. XANES of Pd/Al_2O_3 (Pd K edge): (a) before and (b) after gas phase reduction in H_2, (c) after exposure to air, (d) after suspending in H_2O, (e) before and (f) after the reduction of KNO_3 with H_2 in the aqueous phase, (g) bulk Pd.

The position of the absorption edge in the spectra was determined at the maximum of the first derivative. All spectra were aligned using the edge position of the corresponding bulk metal measured simultaneously with the samples. The scattering cross section of the edge metal was determined from the Victoreen coefficients and the height of the edge was normalized to one. The radial distribution functions were calculated from the EXAFS using standard analysis procedures as described, e.g., in [21]. This included the removal of the background scattering using a third-order polynomial function and a Fourier transformation of the k^2-weighted oscillations over the range $k = 3$–16 $\mathrm{\AA^{-1}}$. The contributions of the first coordination shell were isolated from the Fourier transformed oscillations in the range between $r = 1.35$–3.1 and 1.5–3.2 Å for Cu and Pd, respectively, and analyzed using phase shift and amplitude functions calculated from the corresponding bulk metals. The Pd–Cu and Cu–Pd contributions of the bimetallic catalysts were calculated using the program FEFF (version 8) [22], the data treatment was done with the WinXAS program (version 1.3) [23].

3. Results

The X-ray absorption spectra of the Pd/Al_2O_3 and $PdCu/Al_2O_3$ catalysts measured at the Pd K edge before and after gas phase reduction in H_2, after suspending the catalysts in H_2O and before and after the reduction of KNO_3 with H_2 in the aqueous phase are compared in figures 1 and 2. For the precursors of the Pd/Al_2O_3 and $PdCu/Al_2O_3$

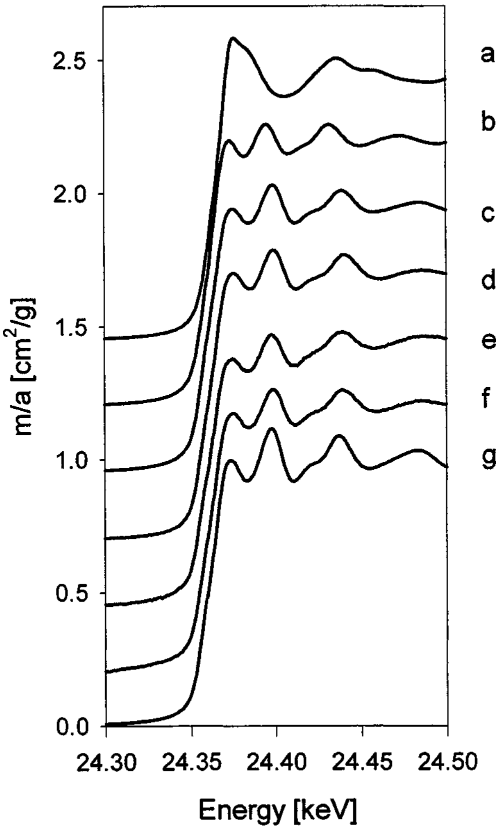

Figure 2. XANES of PdCu/Al_2O_3 (Pd K edge): (a) before and (b) after gas phase reduction in H_2, (c) after exposure to air, (d) after suspending in H_2O, (e) before and (f) after the reduction of KNO_3 with H_2 in the aqueous phase, (g) bulk Pd.

catalysts the intensities of the peaks above the Pd K absorption edge were significantly higher compared to the reduced catalysts, where the XANES observed were essentially the same as those of bulk Pd. For both catalysts further changes in the XANES were not observed after exposing the samples to the aqueous phase and during the nitrate reduction reaction.

The XANES at the Cu K edge of Cu/Al_2O_3 and PdCu/Al_2O_3 before and after reduction with H_2, in the aqueous phase and before and after the KNO_3 reduction reaction are shown in figures 3 and 4. For both catalyst precursors intensive peaks above the Cu K edge were observed, which decreased in intensity during the reduction in H_2. In contrast to the samples measured at the Pd K edge, the XANES of the reduced Cu/Al_2O_3 and PdCu/Al_2O_3 catalysts were not identical after reduction. While the features in the XANES of the reduced Cu/Al_2O_3 catalyst resembled those of bulk Cu, the XANES of the bimetallic PdCu catalyst showed a broader and more intense peak above the absorption edge. These features did not change markedly for both catalysts after exposure to air at 298 K. After contact with the liquid phase a pronounced increase in the intensity of the peak above the absorption edge was observed in the XANES of both samples. Note that after the reduction in the aqueous phase the XANES of the monometallic Cu/Al_2O_3 catalyst resembled that of its oxidic precursor, while the

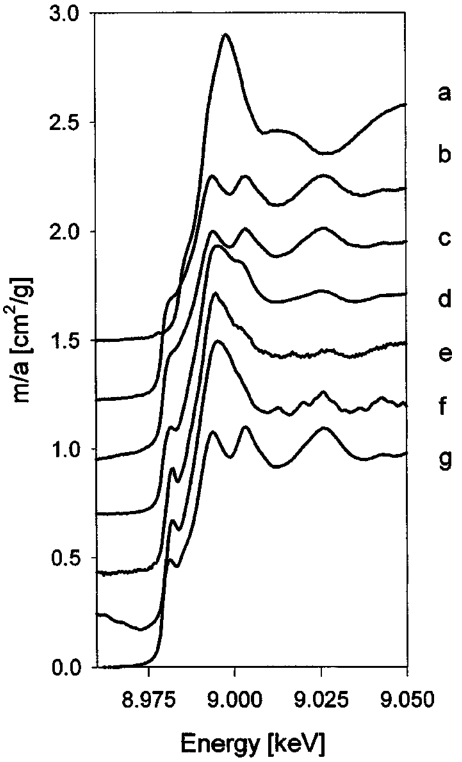

Figure 3. XANES of Cu/Al_2O_3 (Cu K edge): (a) before and (b) after gas phase reduction in H_2, (c) after exposure to air, (d) after suspending in H_2O, (e) before and (f) after the reduction of KNO_3 with H_2 in the aqueous phase, (g) bulk Cu.

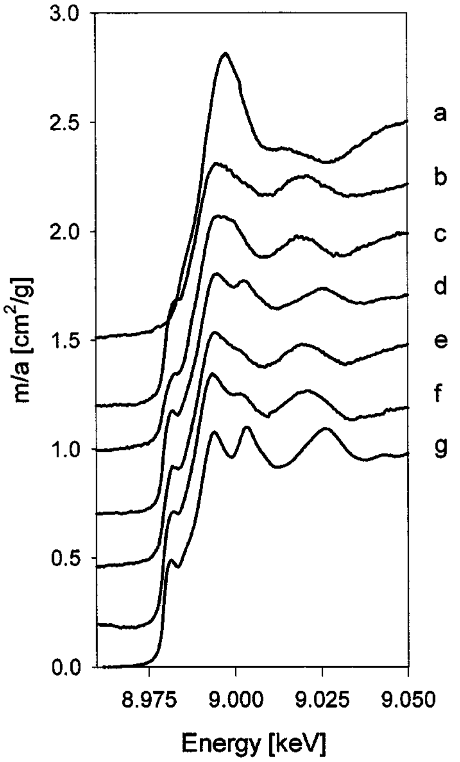

Figure 4. XANES of PdCu/Al_2O_3 (Cu K edge): (a) before and (b) after gas phase reduction in H_2, (c) after exposure to air, (d) after suspending in H_2O, (e) before and (f) after the reduction of KNO_3 with H_2 in the aqueous phase, (g) bulk Cu.

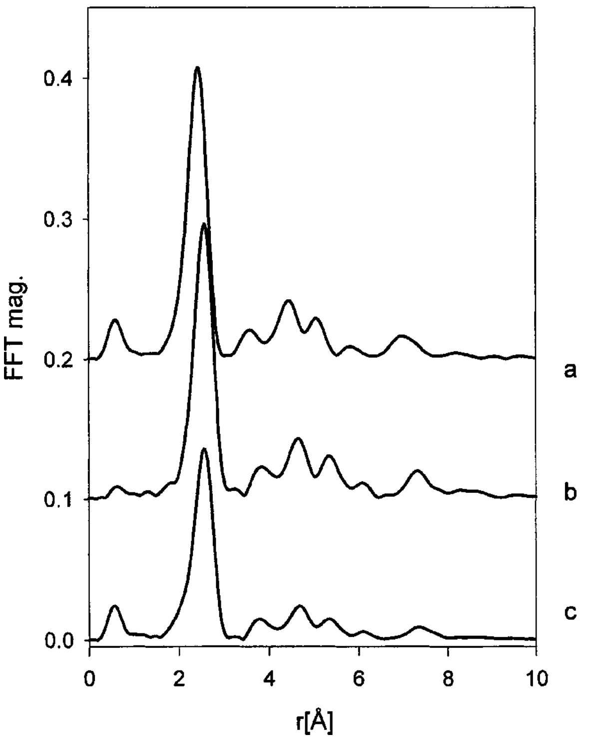

Figure 5. Magnitude of the Fourier transformed EXAFS (Pd K edge): (a) bulk Pd, (b) Pd/Al_2O_3 reduced and (c) $PdCu/Al_2O_3$ reduced.

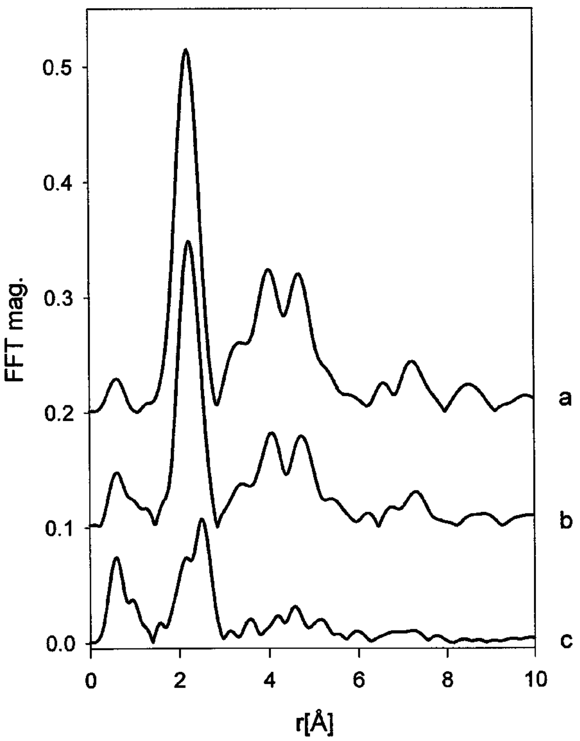

Figure 6. Magnitude of the Fourier transformed EXAFS (Cu K edge): (a) bulk Cu, (b) Cu/Al_2O_3 reduced and (c) $PdCu/Al_2O_3$ reduced.

changes in the XANES of the bimetallic catalyst were less pronounced.

The Fourier transformed EXAFS observed at the Pd and Cu K edges of the reduced mono- and bimetallic catalysts are compared to that of the corresponding bulk metals in figures 5 and 6. The contributions of atoms in the first coordination shells of Pd and Cu are compiled in tables 1 and 2. For both catalysts the Pd–Pd distance ($r_{\text{Pd–Pd}}$) increased from 2.75 to 2.85 Å, which indicates the formation of a β-Pd-hydride phase during the reduction of the catalysts in H_2 [24]. The Cu–Cu distance of the monometallic catalyst was the same as in bulk Cu and increased only slightly due to the presence of the larger Pd atoms in the bimetallic sample. Note, that for the bimetallic catalyst backscattering from Cu atoms was not observed in the EXAFS at the Pd K edge (figure 5(c)), while the radial distribution function of Cu clearly indicated the presence of Cu–Pd contributions for $PdCu/Al_2O_3$ (figure 6(c)). In addition, the quality of the fit could not be improved by using Pd–Cu contributions in the EXAFS analysis of the bimetallic catalyst at the Pd K edge.

Table 1
Results of the EXAFS analysis at the Pd K edge.

Sample	$N_{\text{Pd–Pd}}$	$r_{\text{Pd–Pd}}$ (Å)	$\Delta\sigma^2_{\text{Pd–Pd}}$ (Å^2)
Pd metal (reference)	12	2.751	0
Pd/Al_2O_3	11.0	2.852	6.7×10^{-5}
$PdCu/Al_2O_3$	5.9	2.858	1.8×10^{-4}

4. Discussion

The XANES of a metal oxide is dominated by peaks with high intensity above the X-ray absorption edge, the so-called white line, while these peaks are of lower intensity in the XANES of reduced metals [25]. This difference in the white line intensity between the oxidized and the metallic state is understood in terms of a greater density of unoccupied states near the Fermi-level for oxidized metals and thus can be related to the oxidation state [26,27].

The decrease in the intensity of the peaks above the Pd and Cu K absorption edges after reduction of the catalysts in H_2 at 773 K and the absence of metal–oxygen contributions in the EXAFS indicated the formation of reduced

Table 2
Results of the EXAFS analysis at the Cu K edge.

Sample	$N_{\text{Cu–Cu}}$	$r_{\text{Cu–Cu}}$ (Å)	$\Delta\sigma^2_{\text{Cu–Cu}}$ (Å^2)	$N_{\text{Cu–Pd}}$	$r_{\text{Cu–Pd}}$ (Å)	$\Delta\sigma^2_{\text{Cu–Pd}}$ (Å^2)
Cu metal (reference)	12	2.553	0	–	–	–
Cu/Al_2O_3	9.6	2.551	1.9×10^{-4}	–	–	–
$PdCu/Al_2O_3$	2.4	2.583	1.3×10^{-3}	4.9	2.63	1.5×10^{-3}

metal particles. The similar features in the XANES at the Pd K edge between the reduced Pd/Al_2O_3 and $PdCu/Al_2O_3$ catalysts and metallic Pd reveal the formation of a completely reduced Pd phase in the particles. In contrast, in the XANES at the Cu K edge the peaks were significantly more intense for the bimetallic $PdCu/Al_2O_3$ catalyst, while only the XANES of the monometallic Cu/Al_2O_3 catalyst resembled that of the bulk metal. The differences observed between the XANES of the mono- and bimetallic catalysts at the Cu K edge indicate the formation of a bimetallic PdCu phase. Note that we have already observed a similar trend in the XANES of bimetallic $PtNi/SiO_2$, where with increasing Ni/Pt ratio the intensity of the first peak above the absorption edge increased for Ni and decreased for Pt [28].

The formation of the bimetallic PdCu phase was only observed in the EXAFS at the Cu K edge. Significant Cu–Pd contributions were present in the radial distribution function of the bimetallic catalyst at the Cu K edge and the analysis of the EXAFS indicated an increase in the distance between the Cu atoms due to the lattice expansion resulting from the incorporation of the larger Pd atoms. In contrast, contributions from neighboring Cu atoms were not observed in the radial distribution function of Pd nor were necessary to fit the EXAFS of the bimetallic catalyst observed at the Pd K edge. This is in agreement with the XANES data, where the presence of the bimetallic phase was also only observed at the Cu K edge, while at the Pd K edge no indication of a bimetallic phase was found. Conceptually, X-ray absorption spectroscopy summarizes the contributions of all absorber atoms exposed to the X-ray beam. Due to the significantly higher concentration of Pd in the bimetallic catalyst only a small fraction of Pd atoms appear to be in the direct neighborhood of Cu. Consequently, the contributions from the Pd phase were dominating over the contributions from the bimetallic PdCu phase at the Pd K edge. Furthermore, the formation of the Pd-hydride phase led to an increase in the distance between the Pd atoms, which could be an additional reason why the Pd–Pd and Pd–Cu contributions could not be differentiated in the EXAFS of the bimetallic catalysts. For bimetallic alumina-supported PdCu catalysts an enrichment of the surface of the metal particles with Cu was reported by Molenbroek et al. [16] and Pintar et al. [8]. Therefore, most of the Cu atoms in the bimetallic catalyst should be located in close vicinity of Pd atoms and, thus the changes in the EXAFS of Cu are more pronounced compared to Pd.

Within the limits of accuracy there was no indication for the formation of an oxidic surface layer on Pd for the Pd/Al_2O_3 and $PdCu/Al_2O_3$ catalysts during the reaction in the aqueous phase at 298 K. In contrast, for both Cu catalysts the changes observed in the XANES clearly revealed a partial oxidation of the Cu phase after contact with the aqueous reactant. For the monometallic Cu/Al_2O_3 catalyst a similar oxidation state as in the oxidic precursor was observed after the nitrate reduction in the liquid phase. In the bimetallic catalyst the peak above the absorption edge increased only slightly before and after the nitrate reduction reaction in the aqueous phase, which indicates that the Cu component was only partially oxidized under these conditions. The results clearly showed that under reaction conditions the noble metal component is in a reduced state, while the less-noble metal is partially oxidized. In the monometallic Cu/Al_2O_3 catalysts the metal was strongly oxidized during the reaction, while in the bimetallic catalyst Cu was stabilized in a partially reduced state most likely due to the close contact with the noble metal.

The differences in the XANES of Cu between the mono- and bimetallic catalysts under reaction conditions and the results from the EXAFS analysis for the reduced bimetallic catalysts indicated the formation of Cu rich bimetallic domains, which were preferentially formed on the surface of the metal particles. On these catalysts the noble metal phase was found to be in a reduced state, while the less-noble metal phase was slightly oxidized under reaction conditions. We would like to speculate that the surface polarity induced is favorable for the reduction of nitrates. In principle, the nitrate reduction occurs via two consecutive reaction steps. Only bimetallic catalysts were found to be active for the reduction of nitrate to nitrite, while monometallic noble metal catalysts are only active for the reduction of nitrite to nitrogen [5]. Typically, Pd is combined with less-noble metals, which are, based on the results presented here, in a partially oxidized state. Thus, the noble metal component in the bimetallic catalyst appears to have two functionalities. It is the active phase for the reduction of nitrite to nitrogen and it stabilizes the less-noble metal in a partially reduced phase.

5. Conclusions

The experiments reported clearly revealed that *in situ* experiments in the aqueous phase are necessary to understand the properties of the $PdCu/Al_2O_3$ catalysts during the liquid phase nitrate reduction. Under the reaction conditions studied Pd was found to be in a reduced state in Pd/Al_2O_3 and $PdCu/Al_2O_3$. In the monometallic Cu/Al_2O_3 catalyst Cu was completely oxidized during the contact with the aqueous phase, while in the bimetallic $PdCu/Al_2O_3$ catalyst Cu was stabilized in a partially oxidized state. A PdCu phase was formed in the bimetallic catalyst, which is presumably located in small domains on the surface of Pd rich particles. The noble metal component is the active phase for the nitrite reduction and stabilizes the less-noble metal in a partially reduced state. The polarity generated by the reduced and the partially oxidized metal phases on the surface of the metal particles appears to have a positive effect on the activity of the catalysts for the nitrate reduction.

Acknowledgement

The work was supported by the Fonds zur Förderung der Wissenschaftlichen Forschung under project FWF

P13521 CHE. The XAFS experiments were carried out at HASYLAB, DESY, Hamburg, Germany and supported by the TMR Contract ERBFMGECT950059 of the European Community. We would like to thank J. Frank (TU Wien) for the construction of the liquid phase cells.

References

[1] A. Kapoor and T. Viraraghavan, J. Environ. Eng. 123 (1997) 371.

[2] Y.I. Matanov-Meytal and M. Sheintuch, Ind. Eng. Chem. Res. 37 (1998) 311.

[3] M. Sell, M. Bischoff and D. Bonse, Vom Wasser 79 (1992) 129.

[4] S. Hörold, K.D. Vorlop, T. Tracke and M. Sell, Catal. Today 17 (1993) 21.

[5] G. Strukul, F. Pinna, M. Marella, L. Meregalli and M. Tomaselli, Catal. Today 27 (1996) 209.

[6] A. Pintar, M. Setinc and J. Levec, J. Catal. 174 (1998) 72.

[7] U. Prüsse, M. Hähnlein, J. Daum and K.D. Vorlop, Catal. Today 55 (2000) 79.

[8] J. Batista, A. Pintar and M. Ceh, Catal. Lett. 43 (1997) 79.

[9] A. Pintar, J. Batista, I. Arcon and A. Kodre, Stud. Surf. Sci. Catal. 118 (1998) 127.

[10] B.S. Clausen, H. Topsøe and R. Frahm, Adv. Catal. 42 (1998) 315.

[11] G.H. Via and J.H. Sinfelt, in: *Series on Synchrotron Radiation Techniques and Applications*, Vol. 2, ed. Y. Iwasawa (1996) p. 47.

[12] A.T. Ashcroft, A.K. Cheetham, P.J.F. Harris, R.H. Jones, S. Natarajan, G. Sankar, N.J. Stedman and J.M. Thomas, Catal. Lett. 24 (1994) 47.

[13] A.P. Markusse, B.F.M. Kuster, D.C. Koningsberger and G.B. Marin, Catal. Lett. 55 (1998) 141.

[14] H.H.C.M. Pinxt, B.F.M. Kuster, D.C. Koningsberger and G.B. Marin, Catal. Today 39 (1998) 351.

[15] G.W. Busser, J.G. van Ommen and J.A. Lercher, Stud. Surf. Sci. Catal. 108 (1997) 321.

[16] A.M. Molenbroek, S. Haukka and B.S. Clausen, J. Phys. Chem. B 102 (1998) 10680.

[17] M. Fernandez-Garcia, J.A. Anderson and G.L. Haller, J. Phys. Chem. 100 (1996) 16247.

[18] C. Marquez-Alvarez, I. Rodriguez-Ramos, A. Guerre-Ruiz, G.L. Haller and M. Fernandez-Garica, J. Am. Chem. Soc. 119 (1997) 2905.

[19] A. Jentys, W. Schießer and H. Vinek, Catal. Lett. 47 (1997) 193.

[20] M. Nomura, in: *Series on Synchrotron Radiation Techniques and Applications*, Vol. 2, ed. Y. Iwasawa (1996) p. 93.

[21] K. Asakura, in: *Series on Synchrotron Radiation Techniques and Applications*, Vol. 2, ed. Y. Iwasawa (1996) p. 34.

[22] S.I. Zabinsky, J.J. Rehr, A. Ankudinov, R.C. Albers and M.J. Eller, Phys. Rev. B 52 (1995) 2995.

[23] T. Resssler, J. Phys. IV (1997) 269.

[24] G. Fagherazzi, A. Benedetti, S. Polizzi, A. DiMario, F. Pinna, M. Signoretto and N. Pericone, Catal. Lett. 32 (1995) 293.

[25] G. Meitzner, Catal. Today 39 (1998) 281.

[26] J.C.J. Bart, Adv. Catal. 34 (1986) 203.

[27] M. Englisch, J.A. Lercher and G.L. Haller, in: *Series on Synchrotron Radiation Techniques and Applications*, Vol. 2, ed. Y. Iwasawa (1996) p. 93.

[28] A. Jentys, B.J. McHugh, G.L. Haller and J.A. Lercher, J. Phys. Chem. 96 (1992) 1324.